Search for New Physics with the Atlas detector at LHC

Louis Franck

UFR Sciences et Technologies

Laboratoire de Physique Corpusculaire
de Clermont-Ferrand

MASTERS DEGREE IN SCIENCE OF MATTER
SECOND YEAR

SPECIALTY: Particle Physics

INTERNSHIP REPORT

Search for New Physics with the ATLAS detector at LHC

by

Louis FRANCK

Internship supervisor: **Julien DONINI**

June 2015

Acknowledgments

I would first and foremost wish to thank my internship supervisor: Julien Donini, for his calm and clear explanations, for his patience and for all he has taught me during these few months. I am very lucky and proud to be able to continue this study under his supervision.

Geoffrey has been an always reliable source of physics knowledge and motivation as well, and I would like to thank him too.

I would also like to thank the ATLAS team at Clermont-Ferrand, it has been a real pleasure to be part of such a group during this internship. Their constant readiness to help and talk about physics has been a great motivation and I am sure it will continue like this for the three years to come.

I would like to express my gratitude to the Laboratoire de Physique Corpusculaire of Clermont-Ferrand, and to all the teachers I have had during this Master's degree.

And last but not least, I would like to thank Cecile, for whom words could not be enough to say what I feel.

Contents

Introduction

The twentieth century has seen the birth and explosion of particle physics. New particles were imagined, theoretical models were created, and these were discovered and confirmed by experiment. This success story was turning into chaos considering the number of elementary objects that would compose our Universe, until the 1960s, when the quark model was introduced by Gell-Mann, and a spontaneous symmetry breaking mechanism was constructed by Brout, Englert and Higgs. These models and discoveries have enabled a complete classification of the elementary components of Nature and their interactions, called the Standard Model.

For the last 50 years this model has been tested, and with no real discrepancies so far, all data agree with its' predictions, with very high precision measurements having been made which seem to confirm the theory, plus the discovery of a solid candidate to the Higgs boson in 2012: it is the new era of particle physics' success story.

However, several reasons lead to the belief that this is not the ulimate model, that it is only correct until a certain range of energy, and is thus incomplete. A large number of theories beyond the Standard Model exist, introducing new symmetries, extra dimensions, and predicting new particles... These theories sum up to what is called New Physics.

Top quark physics is seen as an opportunity for probing the Standard Model and searching for New Physics, since the top quark is the heaviest elementary particle (it has a mass roughly 175 times that of the proton). Its' mass and properties could be the gate to new theories, which is why it is the centre of many experiments.

Testing the Standard Model and searching for New Physics are performed in high energy particle colliders, such as the Large Hadron Collider at CERN, in Geneva. This collider is the largest in the world, the one capable of reaching the highest energies and highest frequencies of particle collisions, which makes it a top quark factory. The ATLAS detector at the LHC is a formidable tool for these researches, for it is a complete and general detector, enabling the reconstruction of almost all known particles (all but neutrinos) with the diversity of its' sub-detectors. Moreover, the run II of the LHC is starting this year, in which we will see the collisions' centre of mass energy rise from the previous 8 TeV to an unprecedented 13 TeV, which should create opportunities for finding New Physics.

This study consists in searching for a new particle: the W' boson, through top quark physics, in the ATLAS detector at LHC during run II. Before the data arrives, the studies are made on Monte Carlo simulated data, recreating the events that we should see during run II. Doing so, we will be ready to study the actual data as soon as it arrives. This new particle we are looking for is present in many theories beyond the Standard Model, and could help answer to many questions left open today.

In its' first part, this report briefly describes the Standard Model and some New Physics theories, as well as the LHC and the Atlas detector. We will in the second part go through several studies that have been made during this internship, split into two chapters. We shall first explain our parton level studies and point out physics aspects that will handicap the search for the W' boson, as well as show the increase in potential for its' discovery during run II. In the final chapter, the steps to the reconstruction of the W' boson in a detector will be detailed, and we shall explain the selection criteria that discriminate the researched signal from background processes as well as show the improvements we have looked to bring to these for run II.

Part I

Theoretical and experimental contexts

Chapter 1

Theoretical context

Particle physics' success story is due to the agreement between theory and experimental discoveries. Throughout the nineteenth and twentieth centuries, theories have been made and then confirmed by several experiments, and new discoveries have seen the birth of many new theories, some of them later being confirmed. This constant overlapping was crowned with success many times, and has been the key to our understanding of Nature:

- **1864** J.C. Maxwell announces his formulation of electrodynamics, the earliest field theory having a gauge symmetry;
- **1897** Discovery of the electron by J.J. Thomson;
- **1905** Wave-particle duality is developed and the photon is imagined by A. Einstein;
- **1905** The theory of special relativity is presented by A. Einstein;
- **1911** The Geiger-Marsden experiments of 1909 are analysed by E. Rutherford, who overturns Thomson's model of the atom and presents his own, demonstrating the existence of an atom core, later called nucleus;
- **1915** General relativity is proposed by A. Einstein;
- **1917-19** Discovery of the proton by E. Rutherford (predicted by W. Prout in 1815);
- **1925-26** E. Schrödinger formulates the so-called equation to describe the evolution of a physical system's quantum state;
- **1928** P. Dirac makes the Schrödinger equation relativistic and formulates his own equation, predicting the existence of anti-matter;
- **1930** Prediction of the existence of the neutrino by W. Pauli;
- **1932** Discovery of the first anti-particle, the positron by C.D. Anderson, confirming Dirac's theory;
- **1932** Discovery of the neutron by J. Chadwick;
- **1935-60s** Discovery of more than a hundred new particles, thought to be elementary ones (but in fact were hadrons, made of quarks);
- **1936** Discovery of the muon by C.D. Anderson and S. Neddermeyer;
- **1954** C.N. Yang and R. Mills extend the concept of gauge theory to non-abelian groups to provide an explanation to strong interactions;
- **1956** Discovery of the electron neutrino by C. Cowan and F. Reines, confirming Pauli's prediction;

- **1962** Discovery of the muon neutrino by L.M. Lederman, M. Schwartz and J. Steinberger;
- **1964** M. Gell-Mann, and independantly G. Zweig propose the quark model, solving the number of elementary particles problem;
- **1964** R. Brout and F. Englert, and independantly P. Higgs introduce the spontaneous symmetry breaking mechanism, postulating the existence of a scalar boson, later called Higgs boson;
- **1967** S. Glashow, S. Weinberg and A. Salam unify the electromagnetic and weak interactions and predict the existence of three heavy bosons: $W^{\pm}$ and Z^0;
- **1968** Discovery of the up, down and strange quarks at the Stanford Linear Accelerator Center (SLAC);
- **1973** M. Kobayashi and T. Maskawa theorize the bottom and top quarks, to explain CP violation;
- **1974** Discovery of the J/Ψ meson ($c\bar{c}$ state), and thus the charm quark at SLAC;
- **1975** Discovery of the tau lepton at SLAC;
- **1977** Discovery of the bottom quark at Fermilab;
- **1978** Discovery of the gluon, mediator of the strong interaction, at DESY;
- **1983** Discovery of the $W^{\pm}$ and Z^0 bosons at the Super Proton Synchrotron at CERN;
- **1995** Discovery of the top quark at Fermilab;
- **1998** Discovery of neutrino oscillations, and thus the fact that these have a mass, at the Super-Kamiokande detector;
- **2000** Discovery of the tau neutrino at the DONUT, at Fermilab;
- **2012** Discovery of a candidate to the Higgs boson at the Large Hadron Collider, at CERN.

These theories and discoveries, spread over two centuries, have built the description of particles and their fundamental interactions (with the exception of gravity) as we know it today: the Standard Model.

1.1 The Standard Model

The Standard Model is a theory that relies on a quantum field theory, and more specifically on the concept of gauge invariance. It classifies elementary particles into two main types:
-matter-type particles, of half-integer spin and described by Fermi-Dirac statistics, and
-interaction-type particles (or gauge-type), of integer spin and described by Bose-Einstein statistics. It has a third type, the Higgs boson, which is an essential component of this model since it gives their mass to some of the previous particles thanks to the Brout-Englert-Higgs mechanism.

1.1.1 Matter-type particles

There are 12 elementary matter-type particles in the Standard Model, each one associated to an anti-particle, of same mass and spin but with an opposite electric charge. They can be split into two families:

- **leptons**, integer electric charge (-1 for the charged particles, +1 for their anti-particles and 0 for neutrinos), undergo the Weak interaction and, for charged particles, the Electromagnetic interaction;

- **quarks**, fractional electric charge ($\frac{2}{3}$ for *up* type quarks: u, c and t, and $-\frac{1}{3}$ for *down* type quarks: d, s and b), undergo all three interactions.

In Table 1.1, these particles are split into three families, or generations, the first one represents constituents of ordinary stable matter, whereas the two others are only seen in high energy physics experiments, in colliders or cosmic rays.

Leptons		
Generation	Particle	Mass
First	Electron e	511 keV
	Electron neutrino ν_e	< 2 eV
Second	Muon μ	105.66 MeV
	Muon neutrino ν_μ	< 0.19 MeV
Third	Tau τ	1.777 GeV
	Tau neutrino ν_τ	< 18.2 MeV

Quarks		
Generation	Particle	Mass
First	*up* u	$2.3^{+0.7}_{-0.5}$ MeV
	down d	$4.8^{+0.5}_{-0.3}$ MeV
Second	*charm* c	1.275 ± 0.025 GeV
	strange s	95 ± 5 MeV
Third	*top* t	173.34 ± 0.76 GeV
	bottom b	4.18 ± 0.03 GeV

Table 1.1: Elementary Fermions and their masses [1, 2].

1.1.2 Interaction-type particles

The Standard Model is a quantum field theory, which means it deals with quantum physics and relativity, both needed to describe infinitely small objects. Field theory combines each particle with a field and enables the description of several particles thanks to creation and/or annihilation operators, which enable the description of interactions between these particles.
The Standard Model is also built on the concept of gauge and symmetry invariance, both being linked by Noether's theorem. The lagrangian density describing elementary particles and their interactions must be invariant under certain local-symmetry transformations, called gauge transformations.
This invariance is responsible for the presence of new fields that describe **gauge bosons**.

The Standard Model is based on the following symmetry group:

$$SU(3)_C \otimes SU(2)_L \otimes U(1)_Y$$

where $SU(3)_C$ is the symmetry group for the strong interaction, mediated by **gluons**, and described by Quantum ChromoDynamics [3];
$SU(2)_L \otimes U(1)_Y$ corresponds to the electroweak interaction, combining the electromagnetic interaction, mediated by **photons**, and the weak interaction, mediated by the $W^\pm$ and Z^0 **bosons**, and described by Quantum ElectroDynamics [4,5].
These particles and their masses are summed up in Table 1.2.

Gauge bosons		
Interaction	Particle	Mass
Electromagnetic	photon γ	0
Weak	$W^{\pm}$ bosons	80.385 ± 0.015 GeV
	Z^0 boson	91.188 ± 0.002 GeV
Strong	gluons g	0

Table 1.2: Gauge bosons mediating the fundamental interactions [1].

1.1.3 The Brout-Englert-Higgs mechanism

Up to here, the problem with this theory is that gauge bosons should be massless, which is evidently not the case, as experiments have shown. In 1964, two Belgian theorists Robert Brout and François Englert and a British physicist Peter Higgs, a few months apart, came up with a solution [6–8]: a spontaneous symmetry breaking. This consists in the breaking of the $SU(2)_L \otimes U(1)_Y$ symmetry while keeping a $U(1)_{EM}$ symmetry intact. This mechanism introduces a new doublet of complex scalar fields:

$$\Phi_H = \begin{pmatrix} \Phi^+ \\ \Phi^0 \end{pmatrix}$$

and a (later named) Higgs potential:

$$V(\Phi_H) = -\mu^2 \Phi_H^\dagger \Phi_H + \lambda (\Phi_H^\dagger \Phi_H)^2$$

Searching for the minimum of this potential, the configuration in which $\mu^2 > 0$ leads to a trivial solution ($\Phi_H = 0$) which does not give mass to the W and Z bosons. On the other hand, the case where $\mu^2 < 0$ gives to the potential the shape of a "mexican hat", where the minimum is reached for an infinity of solutions, all leading to a value v, called *vacuum expectation value* (*vev*): $v = \sqrt{\frac{-\mu^2}{2\lambda}}$.
In vacuum, the field breaks the $SU(2)_L \otimes U(1)_Y$ symmetry, taking the particular value:

$$\Phi_H^0 = \sqrt{\tfrac{1}{2}} \begin{pmatrix} 0 \\ v \end{pmatrix}$$

Fluctuations of this field around its' minimum lead to:

$$\Phi_H = \frac{e^{i\eta_a(x)\frac{\tau^a}{2}}}{\sqrt{2}} \begin{pmatrix} 0 \\ v + H \end{pmatrix}$$

where the fields η_a are the massless Goldstone bosons, τ^a are the generators of the $SU(2)$ group (with a=1,2,3), and H is a scalar field corresponding to the so-called Higgs boson.
This field enables the W and Z bosons to acquire a mass, and the photon to keep a null one. It also enables the fermions to acquire a mass which will be proportional to v and to their coupling to the Higgs boson, called Yukawa coupling.

On the 4^{th} of July 2012, the ATLAS and CMS experiments present the discovery [9, 10] of a scalar boson with a mass around 125 GeV and having characteristics which tend to the belief that it is the Higgs boson. Recent studies are made on its' spin, mass and branching ratios. These show evidence of its' scalar behaviour [11, 12], and couplings compatible with the Standard Model [13]. The ATLAS experiment, with the $H \to \gamma\gamma$ and $H \to ZZ^*$ decay channels, has measured its' mass [14]:

$$m_H = 125.5 \pm 0.2\ (stat)\ ^{+0.5}_{-0.6}\ (syst)\ \text{GeV}.$$

1.1.4 The top quark

The top quark has a privileged role in the Standard Model, due to its' high Yukawa coupling (close to 1). It is indeed the particle of the Standard Model which has the highest mass, with many experiments determining this property, as the ATLAS and CMS experiments at LHC, and the DØ and CDF experiments at Tevatron.
The Figure 1.1 presents the first worldwide combination of the results of these measurements with all the data from LHC in 2011 (with $\sqrt{s} = 7$ TeV) and all the Tevatron results.
The measured top quark mass gives the value: $m_{top} = 173.34 \pm 0.76$ GeV.

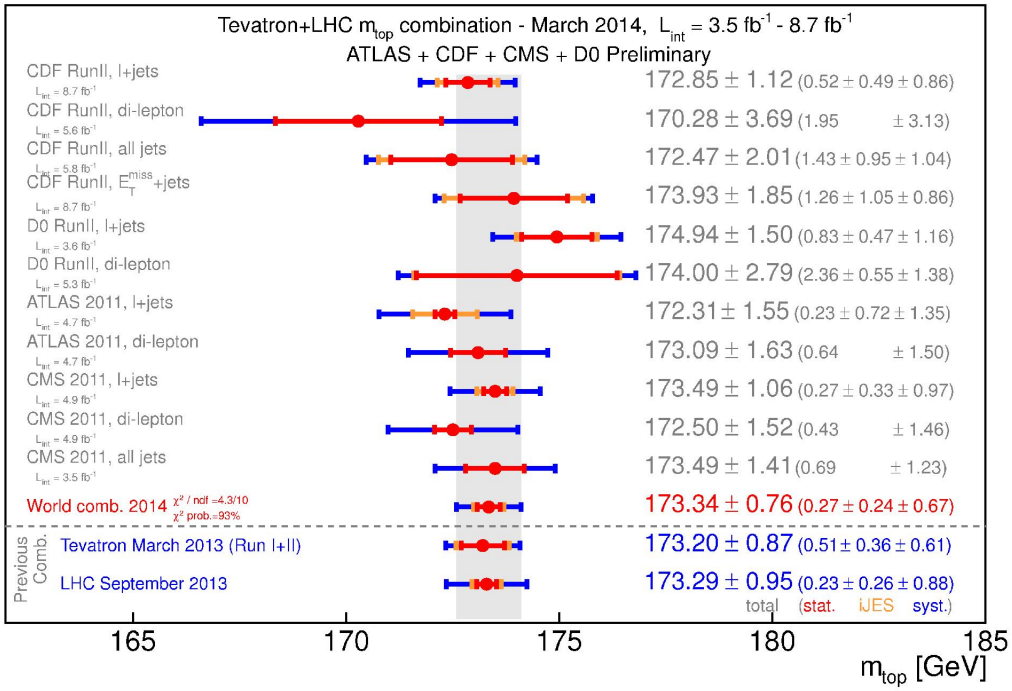

Figure 1.1: ATLAS, CMS, DØ and CDF measurements of the top quark mass, in several decay channels [2].

Moreover, the top quark has a very short lifetime ($\sim 10^{-25}$s [15]), shorter than the time scale at which the strong force of Quantum ChromoDynamics acts ($\sim 10^{-24}$s), thus the top quark decays before it can hadronise. It has thus not been seen as a component of any observed hadron, while other quarks have only been observed as components of hadrons. This makes it very important to know its' production and decay processes.

Several processes in the Standard Model give productions of $t\bar{t}$ pairs, as (a) quark-antiquark annihilation (in $\sim 10\%$ of cases), or (b) gluon fusion (in $\sim 90\%$ of cases) [15]; and of single top quark productions, with different final states for the three production channels: (a) the s channel, (b) the t channel and (c) the tW channel. The corresponding Feynman diagrams are given in Figures 1.2 and 1.3.

The top quark decays in almost 100% of the time to a W boson and a b-quark. Therefore, knowing the final states of the top quark decay is equivalent to knowing those of the W boson, since the b-quark will hadronise in the detector and create a jet. It is possible to determine experimentally whether a jet comes from a b-quark, using dedicated algorithms [16]: this is called "b-tagging".

The W boson can decay hadronically or leptonically, as shown in Table 1.3.

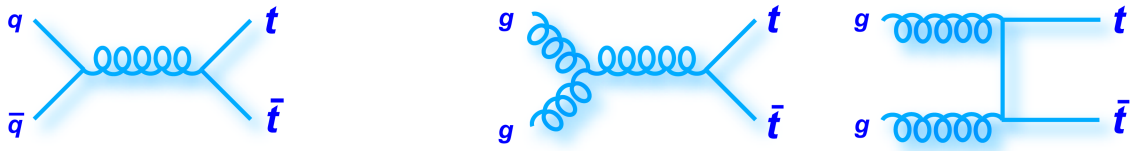

(a) (b)

Figure 1.2: Feynman diagrams for the production of $t\bar{t}$ pairs.

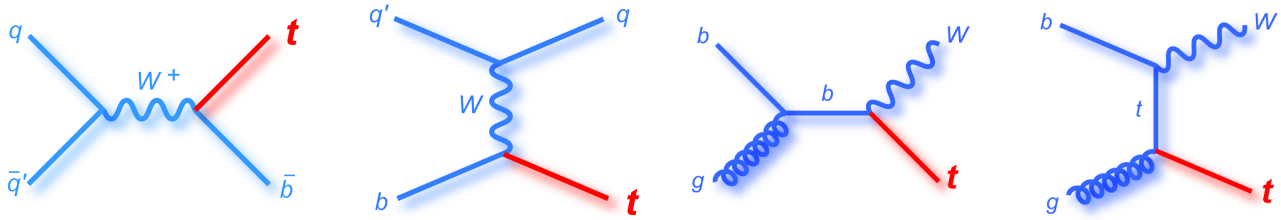

(a) (b) (c)

Figure 1.3: Feynman diagrams for single-top-quark production.

Decay	Channel	Branching ratio
Leptonic	$W \to e\nu$	(10.75 ± 0.13) %
	$W \to \mu\nu$	(10.57 ± 0.15) %
	$W \to \tau\nu$	(11.25 ± 0.20) %
Hadronic	$W \to q\bar{q}'$	(67.60 ± 0.27) %

Table 1.3: Branching ratios of the W boson decays in leptonic and hadronic channels [1].

The top quark, with its' unique properties, has a great role in the search for New Physics. It is indeed the particle of the Standard Model that should have the highest Yukawa coupling, and the highest coupling to new massive particles. In some New Physics theories, it does not owe its' mass to the Higgs boson but to a new boson which would appear with the addition of a $SU(2)$ symmetry group [17–19]. These reasons lead to the search of New Physics through top-quark physics.

1.2 Going Beyond

Though it has many times for the last 40 years been crowned with success with high precision measurements, and its' predictions confirmed by experimental discoveries, several indications lead to the thought that the Standard Model is incomplete and only effective at low energy. It could thus be part of a complete ultimate model which would answer to all the questions left open in particle physics today.

1.2.1 Limits to the Standard Model

The first theoretical limitation concerns gravitation. This is the only known interaction not dealt with by the Standard Model, and even though it is negligible at an energy scale around the electroweak scale (~ 100 GeV), it should be considered at the Planck scale ($\Lambda_p \approx 10^{19}$ GeV). The Standard Model is thus not a valid theory at that scale, and the difference between both energy scales remains unexplained. This is one of its' major problems, called the **hierarchy problem**.

Another problem is the Higgs boson's mass, which would be expected to be very high, because of radiative corrections [20], but experimental constraints and its' recent discovery have lead to a rather low mass. There should thus exist mechanisms that nullify these radiative corrections. This is one example of what is called the **naturalness problem**.

The particle with the highest Yukawa coupling should be the top quark, it should thus be the fermion leading to the most important radiative corrections, though its' coupling to the Higgs boson has not been measured yet.

Another limit to the Standard Model is that it does not predict the existence of dark matter. Its' existence has been confirmed by observations of the rotation curve of several galaxies, which do not match the theoretical predictions, and by the observation of gravitational lensing by huge dark matter concentrations in galaxy clusters, like the Bullet cluster [21].

There are several other examples that weaken the Standard Model, as the fact that it does not explain dark energy, which should amount to roughly 68% of our Universe [22]. In fact, with dark matter amounting to roughly 27%, the Standard Model only describes something around 5% of what our Universe is made of, this clearly points out the Standard Model's incompleteness. Other limits are the unexplained number of families (generations), the *ad-hoc* addition of the BEH mechanism...

1.2.2 New Physics theories

Many theories try to solve these problems, by keeping the Standard Model unchanged at low energy, since nothing yet has proved it wrong, and adding some aspects that could help answer to questions left open today. Most of these theories predict the existence of new particles that have never been observed yet.

The most sought for in general experiments is SUperSYmmetry [20,23], which associates each fermion of the Standard Model to a new boson and *vice versa*. This would extend the internal symmetries of the Standard Model and could solve most of the problems listed above.

There also exist new theories predicting the existence of spatial extra dimensions. One of these is the Kaluza-Klein model [24,25], in which new particles exist as excitations of the Standard Model particles in these extra dimensions. These theories had the initial purpose of attacking the hierarchy problem, by introducing gravitons which would mediate the gravitational interaction and would propagate in these extra dimensions. They could also solve other issues as well, as for instance the existence of dark matter [26], and could offer a solution to the flavour puzzle [27].

Other New Physics theories exist, as the Grand Unified Theories [28] which also extend internal symmetries of the Standard Model, and more [29], some having been invalidated by the discovery of the Higgs boson.

1.2.3 The W' boson

Many of the theories beyond the Standard Model introduce new charged vector currents mediated by heavy gauge bosons, usually called W'. It will appear in any theory that introduces a new $SU(2)$ doublet. The invariance of the lagrangian under the new symmetry introduced by this group will be responsible for the presence of a new field, describing a new charged gauge boson. Many New Physics theories introduce this new symmetry, hence our search for the W' boson. For example, this new particle can appear in theories with universal extra dimesions, such as Kaluza-Klein excitations of the Standard Model W boson [30–32], or in theories that extend fundamental symmetries of the Standard Model and introduce a right-handed counterpart to the W boson [33,34].

Little Higgs theories also predict a W' boson [35], which would participate to mechanisms aiming to nullify the quadratic divergences in the Higgs boson's mass computation, and could thus solve the naturalness problem. There are other theories that introduce this new particle, for instance topflavour models [17–19], which seek to explain the high mass of the top quark with the W' boson, by introducing a new $SU(2)$ doublet that would only couple to particles of the 3^{rd} generation (top, bottom, τ, ν_τ).

In this study, we search for a W' boson decaying to a top quark and a b-quark, as shown in Figure 1.4, since several theories beyond the Standard Model expect the W' boson to have a greater coupling to the third generation of quarks than to the first and second, plus it explores models potentially inaccessible to searches for a W' boson decaying into leptons [36–38]. In the right-handed sector, the W' boson can indeed not decay to a charged lepton and a right-handed neutrino if the latter has a mass greater than that of the W' boson.

Searches for a W' boson decaying to a $t\bar{b}$ final state (or $\bar{t}b$) have been performed at the Tevatron [39, 40] in the leptonic top quark decay and at the Large Hadron Collider in both the leptonic [41, 42] and fully hadronic final states [43], excluding right-handed W' bosons with masses up to 2.05 TeV at 95% confidence level.

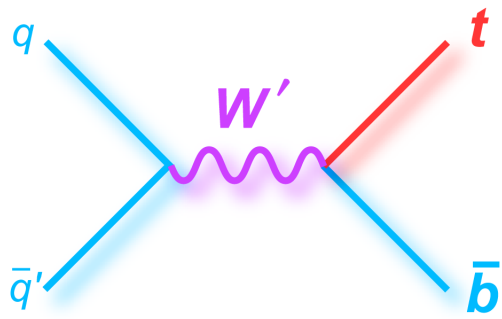

Figure 1.4: Feynman diagram of the production of a W' boson decaying to a $t\bar{b}$ final state.

This particle we are searching for would have a high mass, and will thus require very high energy experiments to be sought for. In the next chapter, we will introduce the Large Hadron Collider, which is the best laboratory for these experiments in the world today, and one of its' four main experiments, specialised in top-quark physics and in the search for New Physics: ATLAS.

Chapter 2

Experimental context

Confirming theoretical models or dicovering new particles requires high energy experiments. In the 1930s, physicists used a unlimited and free source of high energy particles: cosmic rays. The problem with this source of particles is that there is no control of their energy, hence the creation of particle colliders, which were at first small machines, but the need for reaching high energies has created the need for building longer accelerators, thus larger colliders.

These gigantic machines are made of very long tubes in which the particles are accelerated, and large detectors around where the collisions take place. Two types of colliders have been built, linear and circular ones, the latter enabling higher energies to be reached, since the particles are accelerated for several "laps" before reaching the maximum possible energy, which is when the two beams are made to meet and the collision takes place. In these colliders, millions of particles go at ultra high speed. These experiments have enabled the discovery of many particles, as shown in the introduction to chapter 1. All fermions have been discovered in the U.S.A, while all bosons have been discovered in Europe.

2.1 The Large Hadron Collider

The LHC at CERN in Geneva is an underground ring 27 kilometres in circumference and is the largest and most powerful collider up to date. It is a proton-proton collider which could reach energies up to 8 TeV in 2012, and its' run II which is currently starting will enable to reach energies up to 13 TeV. Furthermore, it hosts a very high frequency of collisions ($\sim$ 600 million inelastic events per second), which is interesting for the search of New Physics, since the processes have very low probability. This collider has enabled the discovery of the Higgs boson in 2012, and this unprecedented energy scale brings the exciting prospect of finding New Physics in the coming years. In this collider, four main experiments take place: ALICE, ATLAS, CMS and LHCb.

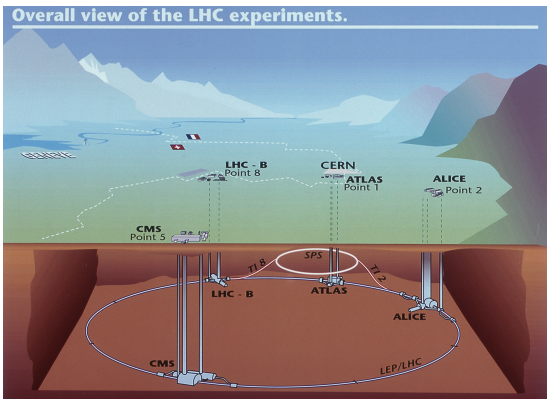

Figure 2.1: Diagram showing the LHC and its' four main experiments.

2.2 A Toroidal LHC ApparatuS

The ATLAS detector at the LHC is the world's largest detector, being almost 45 metres long, more than 25 metres high, and weighing roughly 7000 tons. It is about half as big as the Notre Dame Cathedral in Paris and weighs about the same as the Eiffel tower. It is a multi-purpose detector with roughly 4π coverage, in which around 30 million collisions take place every second, it only records a fraction of the corresponding data, relying on a triggering system.

2.2.1 Sub-detectors

ATLAS is a general detector and thus needs to be exhaustive in terms of particle detection and identification. To identify a particle, the information needed is its' charge, which is obtained by bending the particle's trajectory (if non-zero), and mass, which is obtained by measuring its' momentum and energy. Hence ATLAS' many sub-detectors, as shown in Figure 2.2, capable of interacting with almost every known particle (except neutrinos):

- the inner detector which combines high resolution pixel detectors at the inner radii and continuous tracking elements at the outer radii, for measuring the momentum of charged particles;
- the electromagnetic and hadronic calorimeters, which measures the energies carried by charged and neutral particles;
- the muon spectrometer surrounding the calorimeters, for identifying and measuring the momenta of muons;
- the solenoid magnet system, bending charged particles' trajectory for momentum measurement, and toroid magnets for bending muons' trajectory for precise measurements of their momentum.

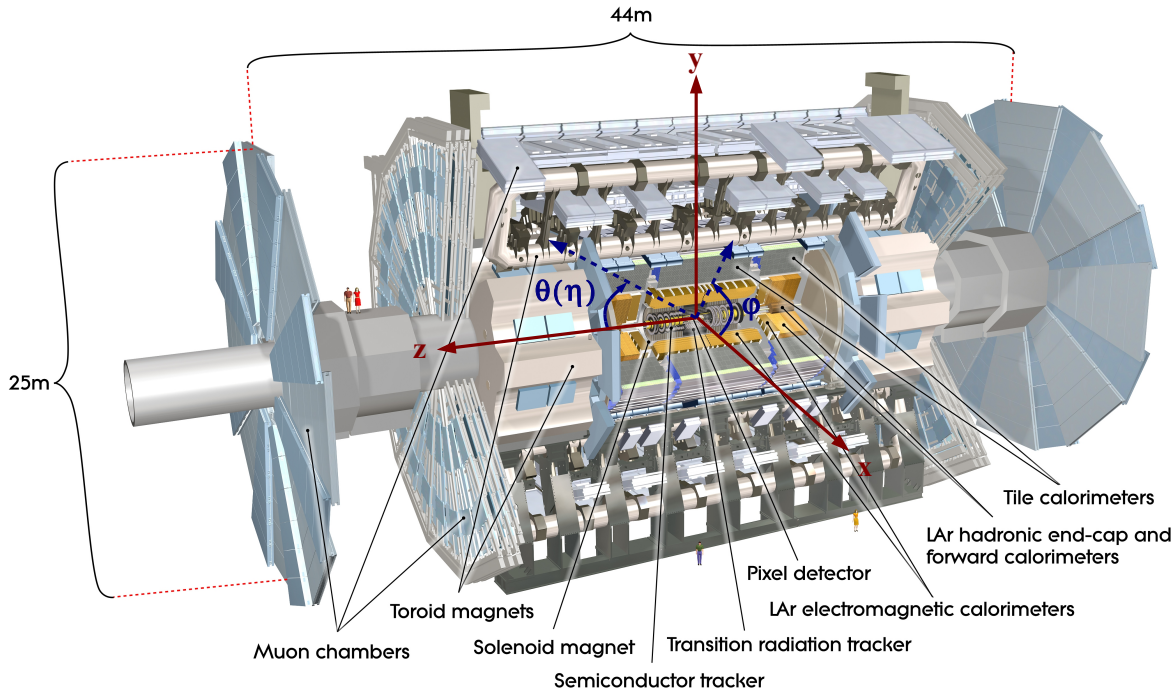

Figure 2.2: The ATLAS detector, with its' many sub-detectors and coordinate system.

2.2.2 Coordinate system

All ATLAS sub-detectors share the same coordinate system, its' origin being the interaction point. The z-axis runs along the beam line, the x-y plane is perpendicular to the beam line and is referred to as the transverse plane. The x-axis points to the centre of the LHC ring and the y-axis points upward to the surface of the earth. The transverse plane is often described in terms of r-ϕ coordinates, the radial dimension r being the distance to the beam line, and the azimuthal angle ϕ being measured from the x-axis, around the beam. The polar angle θ is defined as the angle from the z-axis as shown in Figure 2.2, but is reported in terms of pseudo-rapidity, defined as:

$$\eta = -\ln\tan(\tfrac{\theta}{2})$$

This new coordinate enables to overcome the unknown longitudinal acceleration component: partons interacting in a hadronic collider only carry an unknown fraction of the proton's energy, which can lead to a collision asymmetry and resulting objects not being at rest in the detector reference frame. This is called *boost*. The pseudo-rapidity difference $\Delta\eta$ is *boost* invariant.

The distance ΔR in $\eta - \phi$ space is defined as:

$$\Delta R = \sqrt{\Delta\phi^2 + \Delta\eta^2}$$

and will be used several times in the following studies.

Variables in the transverse plane are also very interesting to consider. The protons in the initial state are indeed accelerated along the z-axis, there is no energy in the transverse plane and thus these variables are not *boosted*. Furthermore, energy conservation enables to reconstruct a neutrino's transverse momentum with a vector sum. We will thus often look at variables in the transverse plane in these studies: p_T and E_T.

We have in this first part had a brief overview of the Standard Model, of its' very precise predictions, but also its' limits. We have furthermore presented a non exhaustive list of New Physics theories, and especially some in which a W' boson appears. Finally we have presented the LHC, the best laboratory to seek for New Physics, and the ATLAS detector, its' completeness making it one of the best tools for top-quark physics and thus for our search.

We will now present our studies of data samples which simulate events like the ones we shall witness in the ATLAS detector during run II.

Part II

Searching for the W' boson

Chapter 3

Parton level studies

The run II of the LHC is currently starting, and this new run will see centre of mass energies of proton-proton collisions rise from 8 to 13 TeV. This unprecedented energy is expected to enable many improvements to already made measurements, as well as bring many new discoveries. It has thus been impatiently waited for. For instance, measurements of the Higgs boson's properties and those of the top quark will be made with higher precision, and the top quark's coupling to the Higgs will probably be measured. Finding New Physics is the other mouth watering prospect of the post-Higgs era, many theories predicting that it should be found at the TeV energy scale.

The studies performed during this internship can be split into two main parts: parton level studies, which we shall describe in this chapter, and the reconstruction of the W' boson from the final state, which will be described in chapter 4. Before the arrival of the LHC run II data, we have prepared ourselves by studying Monte Carlo simulated data, recreating the physical processes, as the Feynman diagram shown in Figure 1.4, as well as the detector response to the particles in the final state.

3.1 Monte Carlo tools

A Monte Carlo simulation of a collision event such as those seen in the Atlas detector is built using a number of generated physics aspects:
- parton distributions, combined with matrix elements at tree-level, also called leading order;
- initial and final states parton showering and hadronisation;
- the detector response.

Three Monte Carlo generators, MadGraph5, Pythia8 and Delphes3, have enabled the creation of data samples on which the studies in this internship have been done.

MadGraph5 [44] is a framework that aims at providing all the elements necessary for Standard Model and New Physics phenomenology, such as the computation of cross sections, the generation of hard events and their matching with event generators, and the use of a variety of tools relevant to event manipulation and analysis.

Pythia8 [45] is a programme for the generation of a number of physics aspects, including hard and soft interactions, parton distributions, initial and final states parton showers, multiparton interactions, fragmentation and decay. It is used in our study to generate parton showering and hadronisation, after the generation of the hard process with MadGraph5.

Delphes3 [46] is a framework for fast simulation of a generic collider experiment. It does not simulate a specific detector but a simple and general one, which includes a tracking system, embedded into a magnetic field, calorimeters and a muon system. The framework is interfaced to standard file formats and outputs observable such as isolated leptons, missing transverse energy and jets which can be used for dedicated analyses. The simulation of the detector response takes into account the effect of the magnetic field, the granularity of the calorimeters and sub-detector resolutions.

3.2 Objectives of the studies

In these studies, we will look at what is called "Truth". This part of the simulated data contains every particle that appears in every event, which sums up to hundreds, even thousands of particles for a highly energetic collision like those that will happen during run II. These particles will be sorted in a tree, with a set of information on them, as their 4-vector, thus kinematical and angular variables, but also their "parent" (the particle which decayed into or radiated this particle), and many more useful characteristics. By studying this dataset, we can look at many different aspects of the event, as the impact of parton distribution functions and of gluon emissions on the quarks' kinematic variables, which will be detailed in this chapter, and the comparison between reconstruction of particles and their "Truth", which is detailed in chapter 4.

Our aim in these studies is to look at the invariant mass of the $\{\text{top}+\bar{b}\}$ system: m_{tb}^{Truth}, in order to obtain the impact of physics phenomena on the W' mass we will reconstruct, by taking the quadri-vectors of the top and b-quarks coming from the W' boson decay. We shall see hereafter the impact of parton distribution functions and of gluon emissions on m_{tb}^{Truth} and have information on the difficulties these aspects will bring to the reconstruction of the W' boson.

3.3 Parton distribution functions

When a collision takes place between two protons, it does not actually take place between these two protons, but between two partons. A proton contains three valence partons: two up quarks and a down quark, but these are not the only partons that can be seen in the proton, there are also the **sea-level partons**. These have a probability of carrying some of the proton's momentum, which has a density called the **parton distribution function**. The cross-section of the process $pp \rightarrow W'$ can be given using the **factorisation theorem**, and will depend on the parton distribution functions.

Figure 3.1 (a) shows different parton distribution functions in the proton at a resolution scale $Q^2 = 10^4\ GeV^2$. This represents the probability density of finding a parton with a given fraction of the proton's momentum with a resolution scale provided by an external probe, such as a virtual photon with virtuality Q^2. In this figure, the parton distribution functions are multiplied by the momentum fraction to suppress the rise at low fractions and for the gluon it is divided by 10 for display purposes.

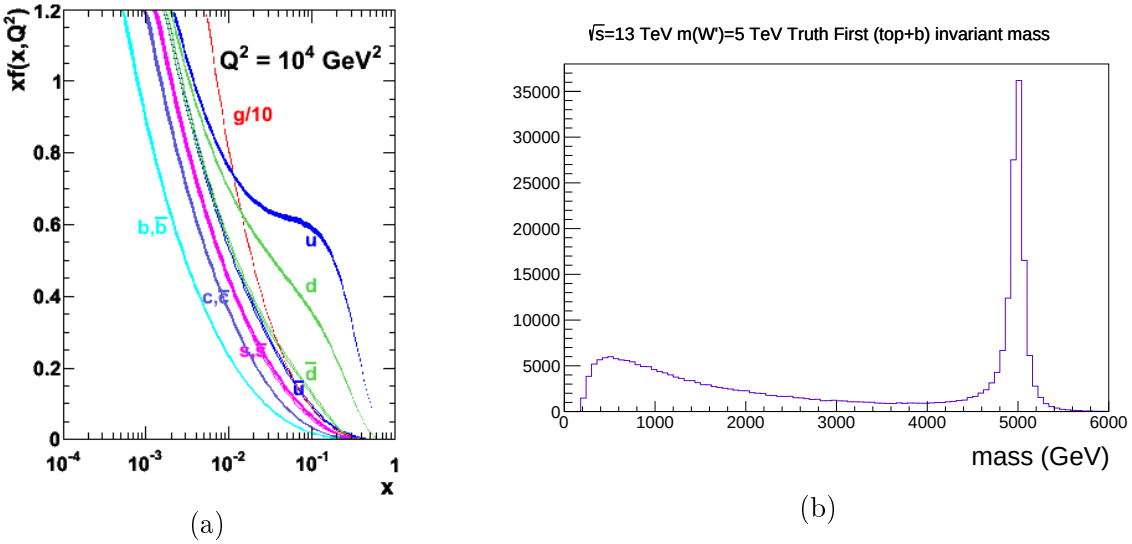

(a) (b)

Figure 3.1: (a) MSTW 2008 next-to-leading order parton distribution functions as a function of the momentum fraction x, at $Q^2 = 10^4\ GeV^2$ [47]. (b) Invariant mass distribution m_{tb}^{Truth} at $\sqrt{s} = 13$ TeV, m(W')=5 TeV.

At a higher resolution scale, thus at higher energy, the partons will have a much higher probability of having a low fraction of the proton's momentum. This effect can be directly witnessed in the invariant mass distribution shown in Figure 3.1 (b), the mass spectrum at a W' mass of 5 TeV is not a Breit-Wigner function, since the effect of the parton distribution functions shift it to lower masses. The mass spectrum is a convolution of a Breit-Wigner function and the parton distribution functions.

3.4 Impact of gluon emissions

The particles that appear the most in an event are gluons. These are constantly interacting with quarks: gluons can be emitted by quarks and can decay into quark-antiquark pairs. Quarks lose some of their energy each time they emit a gluon, and thus when we reconstruct particles by starting from the final state there is an energy loss. This is true at the parton level study, but in a detector a quark is not seen on its' own, it hadronises and is seen as a jet of particles. With the information supplied by the detector, jets are reconstructed as cones, in which there is some of the energy loss due to gluon emissions before hadronisation. Nevertheless, these gluon radiations remain an issue, since in a massive W' decay, the emitted top and $\bar{b}$ will be highly energetic, and will thus emit more gluons, and lose a larger amount of energy.

We have illustrated this in Figure 3.2, with events at $\sqrt{s} = 13$ TeV and W' masses of 1 TeV and 5 TeV, which represents the mean energy loss by the b-quarks which come from the W' decay: $b_{W'}^{Truth}$, due to gluon emissions. As we can see in this figure, the b-quarks have lost a great amount of energy because of these emissions, especially for a high mass of the W' boson.

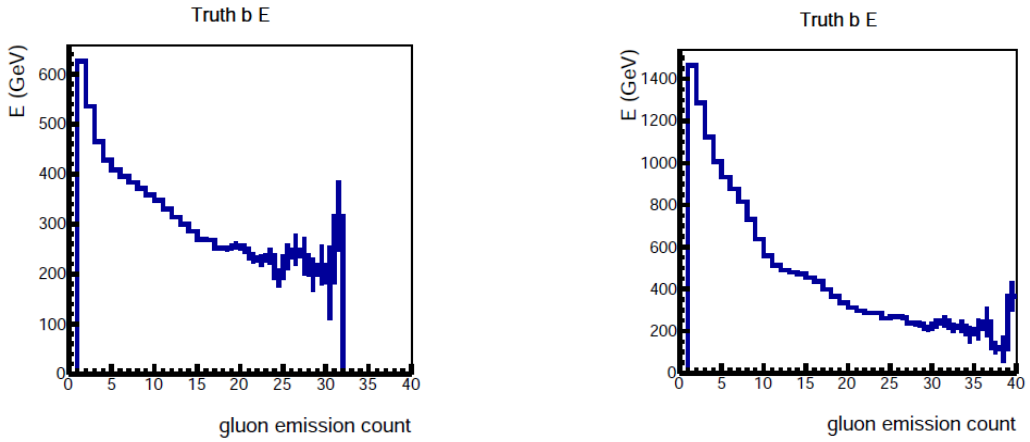

(a) (b)

Figure 3.2: Impact of gluon emissions on the $b_{W'}^{Truth}$ energy at (a) m(W')=1 TeV, (b) m(W')=5 TeV, $\sqrt{s} = 13$ TeV.

This turns out to be a problem when we want to reconstruct the mass of the W' boson, we will obtain a mass far below what it should be. The mass spectrum of the particle should be represented by a Breit-Wigner function, but this is no longer the case, this distribution is shifted to lower masses due to the emissions. An illustration of this issue is shown in Figure 3.3, where the m_{tb}^{Truth} distribution is drawn for W' masses from 1 to 5 TeV (a) before gluon emissions by the top and b-quarks, and (b) after emissions.

Some of these emitted gluons will stay close to the quark, and will thus be part of the jet when the quark hadronises. This means that not all the energy will be lost, though we do not know what proportion of the emitted gluons will be part of the jet, and so we cannot really quantify the energy loss by the quarks.

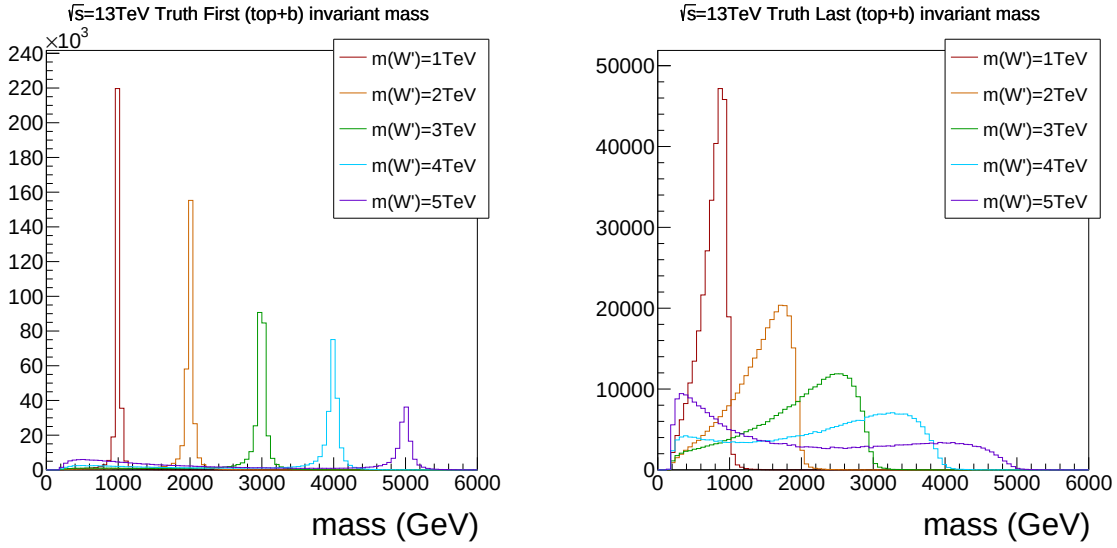

(a) (b)

Figure 3.3: Invariant mass distribution m_{tb}^{Truth} (a) before gluon emissions and (b) after emissions, for W' masses from 1 to 5 TeV at $\sqrt{s} = 13$ TeV.

3.5 A new opportunity!

The probability of producing a massive particle will increase with the energy of the protons in the collision, which is why run II brings a new opportunity for the discovery of the W' boson. In this study, we have pointed out two comparisons of centre of mass energies $\sqrt{s} = 8$ TeV and $\sqrt{s} = 13$ TeV which show this increased probability. We have drawn invariant mass distributions, and looked at the $q\bar{q}' \to W' \to t\bar{b}$ cross-sections.

3.5.1 Invariant mass distributions

To illustrate the increased potential for discovery of the W' boson, in Figure 3.4 we have drawn histograms of the m_{tb}^{Truth} spectra at centre of mass energies $\sqrt{s} = 8$ TeV and $\sqrt{s} = 13$ TeV.

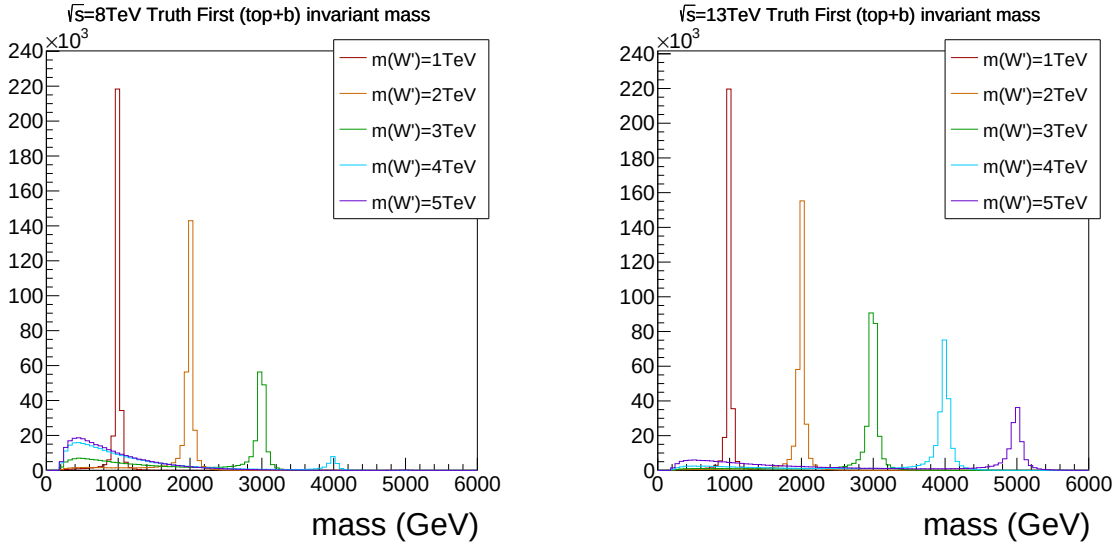

(a) (b)

Figure 3.4: Invariant mass distribution m_{tb}^{Truth} at (a) $\sqrt{s} = 8$ TeV and (b) $\sqrt{s} = 13$ TeV for W' masses from 1 to 5 TeV.

In these histograms, we can see that the shape of the spectrum for W' masses of 3 TeV and higher is not peaked for $\sqrt{s} = 8$ TeV. This is what was expected, since a centre of mass energy of 8 TeV is not sufficient to produce a W' boson with a 4 or 5 TeV mass. This is a direct consequence of the factorisation theorem and of the parton distribution functions explained earlier, since to produce a W' boson there needs to be an interaction between a quark and an anti-quark. The anti-quark will necessarily be a sea-level parton of the proton, thus there is lower probability for it to have a large fraction of the proton's momentum. The parton distribution function has more importance than the Breit-Wigner function for $\sqrt{s} = 8$ TeV and the is thus hardly a convolution. A rise of the protons' energy will of course imply the same for their partons, thus the higher probability of producing a W' boson with a mass of 4 or 5 TeV at $\sqrt{s} = 13$ TeV.

3.5.2 $pp \to W' \to t\bar{b}$ cross-sections

Another point of interest is the probability of production of the signal we are looking for. We have done this by drawing in Figure 3.5 the theoretical leading order (LO) cross-sections of the $pp \to W' \to t\bar{b}$ process at both centre of mass energies, and also the ratio of these, giving an idea of the increased potential.

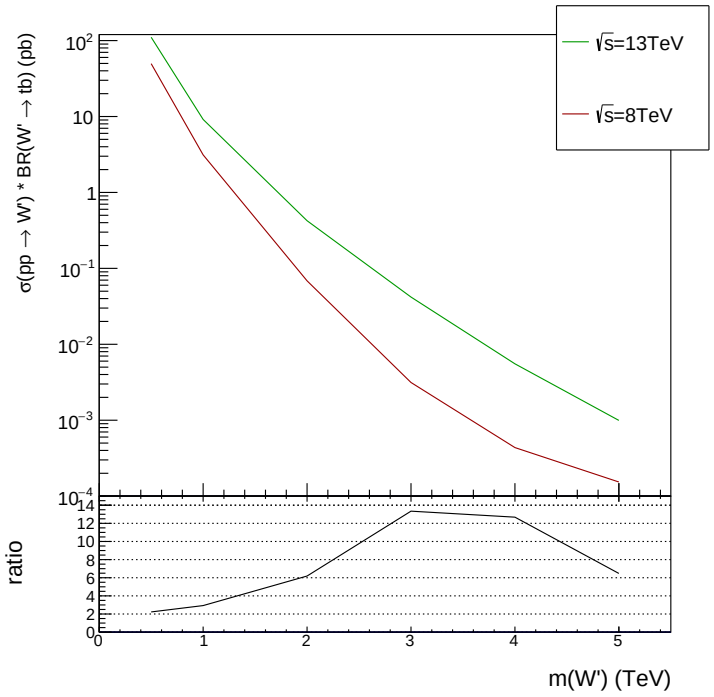

Figure 3.5: Theoretical cross-sections at $\sqrt{s} = 8$ and 13 TeV and their ratio, for W' masses from 0.5 TeV to 5 TeV.

These cross-sections correspond to theoretical predictions calculated using MadGraph5. This figure shows that the probability of producing a W' with a mass of 3 or 4 TeV will be multiplied by a factor 13. The ratio decreases for higher masses due to the parton distribution functions, at higher energies there is a higher probability of finding a parton with a low fraction of the proton's momentum, which has an impact on the process cross-section.

Chapter 4

Searching for $W' \rightarrow tb$ events

In this study, we have also used simulations of the detector's response to the particles passing through it. For this, we have used DELPHES. The generated data enabled us to reconstruct events corresponding to the researched signal the same way we shall do during run II. This reconstruction is an indirect one, we have a given final state and obtain the W' boson proceeding step by step, by building the 4-vector of each particle in our process.

4.1 Procedure

In this procedure, we will reconstruct at the detector level every particle seen in the Feynman diagram in Figure 4.1, from the final state to the W' boson. Our search of this particle is done in the leptonic final state, for a simpler identification and to limit backgrounds, which we shall detail in this chapter. The final states we will consider consist in two b-jets, a lepton and missing transverse energy (E_T^{miss}), corresponding to the neutrino.

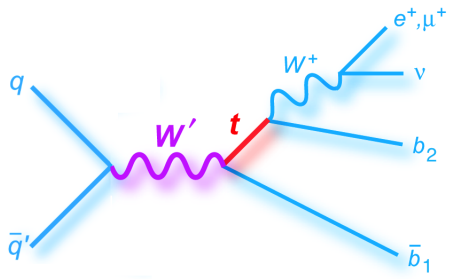

Figure 4.1: Feynman diagram of the searched W' process, in the leptonic final state.

4.1.1 Building the neutrino 4-vector

First of all, we need to build the neutrino 4-vector, this particle being in the final state but not interacting in the detector, so it is not seen. The only available information is the missing transverse energy, since in the initial state the protons are accelerated along the z-axis, there is no momentum in the transverse plane. Energy conservation requires for the final state to be the same, all vectors in the transverse plane must sum up to zero. If this is not the case, there should be a neutrino in the process, and we obtain its' transverse momentum by drawing the vector that makes the sum go to zero. The problem is we cannot do the same along the z-axis, since we do not know what proportion of the proton's momentum each parton has. We can only postulate that: our interaction being between a quark, a valence parton, and an antiquark, a sea-level parton, the quark will carry more momentum and thus the sum of momentas along the z-axis will not be null.

We must thus build the neutrino's longitudinal momentum: $p_{z,\nu}$. To do so, we use the fact that the neutrino and charged lepton come from the decay of the W boson, which has a known mass of 80.385 ± 0.15 GeV. We use this mass as a constraint to obtain a quadratic equation:

$$p_{z,\nu}^2 - \frac{p_{z,l}(m_W^2 - m_l^2 + 2A)}{E_l^2 - p_{z,l}^2} p_{z,\nu} + \frac{E_l^2 p_{T,\nu}^2 - \left(\frac{m_W^2 - m_l^2}{2} + A\right)^2}{E_l^2 - p_{z,l}^2} = 0 \tag{4.1}$$

where p represents the momentum and E the energy, l is the charged lepton, and $A = \overrightarrow{p_{T,l}}.\overrightarrow{p_{T,\nu}}$ is the scalar product between the momentum of the neutrino and of the lepton in the transverse plane. This equation leads to the solution:

$$p_{z,\nu} = B \pm \sqrt{\Delta} \tag{4.2}$$

$$\text{with: } B = \frac{p_{z,l}\left(\frac{m_W^2 - m_l^2}{2} + A\right)}{E_l^2 - p_{z,l}^2} \quad \text{and} \quad \Delta = B^2 - \frac{E_l^2 p_{T,\nu}^2 - \left(\frac{m_W^2 - m_l^2}{2} + A\right)^2}{E_l^2 - p_{z,l}^2}.$$

In the case where $\Delta > 0$, we have decided to choose the solution with lowest longitudinal momentum, but as we see in Figure 4.2, there is not a great difference, except that by taking the maximum all null solutions disappear. This figure confirms our choice of the minimum, but we could probably keep both, as two solutions for the W boson, which could be useful for the next step.

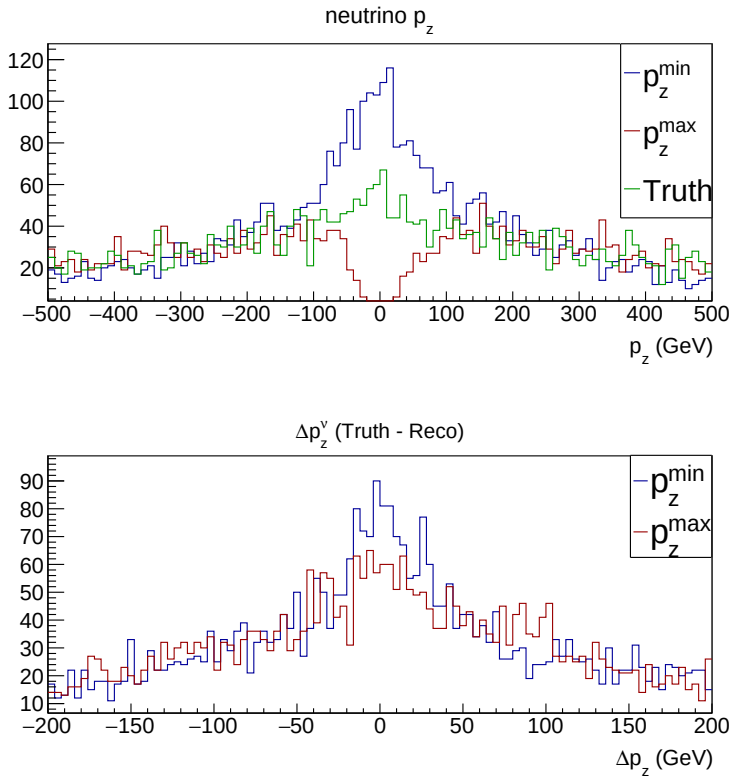

Figure 4.2: Comparison of the calculated $p_{z,\nu}$ to the "Truth" in the case where $\Delta > 0$, we choose to take the lowest and highest longitudinal momenta, $\sqrt{s} = 13TeV$, m(W')=3 TeV.

In the case where $\Delta < 0$, we would obtain an imaginary solution. In this case there could be an imperfect resolution of the missing transverse energy measurement, and so we modify it for Δ to become null.

We do so by obtaining a polar equation, between $||\overrightarrow{p_{T,\nu}}||$ and ϕ. A null discriminant in our quadratic equation will give:

$$p_{T,\nu} = \frac{m_W^2 - m_l^2}{2(\sqrt{E_l^2 - p_{z,l}^2} - p_{T,l} cos\Delta\phi)} \tag{4.3}$$

with $\Delta\phi = \phi_\nu - \phi_l$.
We thus progressively rotate the neutrino's transverse momentum a hundredth of degree at a time, from $\phi_{E_T^{miss}} - 60$ degrees to $\phi_{E_T^{miss}} + 60$ degrees and obtain for each step a norm given by the equation (4.3). We will thus obtain 12000 solutions and choose the one closest to the vector of the measured missing transverse energy.

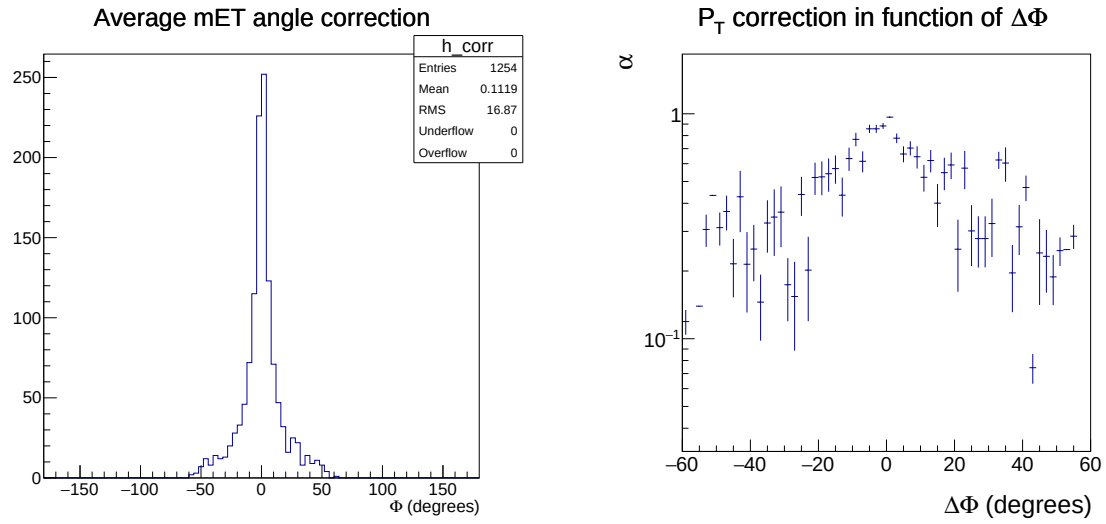

(a) (b)

Figure 4.3: (a) Average angle correction and (b) average norm versus angle correction of the missing transverse energy at $\sqrt{s} = 13$ TeV and m(W')=3 TeV.

Figure 4.3 shows (a) the average angle corrections brought to E_T^{miss}, and (b) the average norm correction: $\frac{p_{T,\nu}}{E_T^{miss}}$ for each angle correction (here $\Delta\Phi$) when the discriminant to equation (4.1) is negative. As seen in this figure, the corrected values are always smaller than the measured ones.

Figure 4.4 shows the comparison of the result to this program: $p_{z,\nu}$ to the "Truth", for a W' mass of 5 TeV, and $\sqrt{s} = 13$ TeV.

4.1.2 Reconstructing the top quark

Once the neutrino 4-vector is built, we obtain the W boson 4-vector by adding the neutrino and charged lepton 4-momenta: $P_W = P_\nu + P_l$. Then, to reconstruct the top quark, we need to find the b-jet corresponding to its' decay: b_{top}.

This is done by choosing, of all the jets in our event, the jet which will give a mass of the system {jet+W} closest to that of the top quark (in the Monte Carlo input: $m_{top} = 172.5$ GeV). Once this jet has been picked, we can build our top-quark 4-vector: $P_{top} = P_W + P_{b_{top}}$.

Figure 4.5 shows the reconstructed top mass at $\sqrt{s} = 13$ TeV and for a W' boson mass of 5 TeV. This mass distribution has a long tail, and as we will see in section 4.2, this way of finding b_{top} is not very effective. Other ways of finding this jet should probably be considered for a better reconstruction of the top quark and thus of the W' boson.

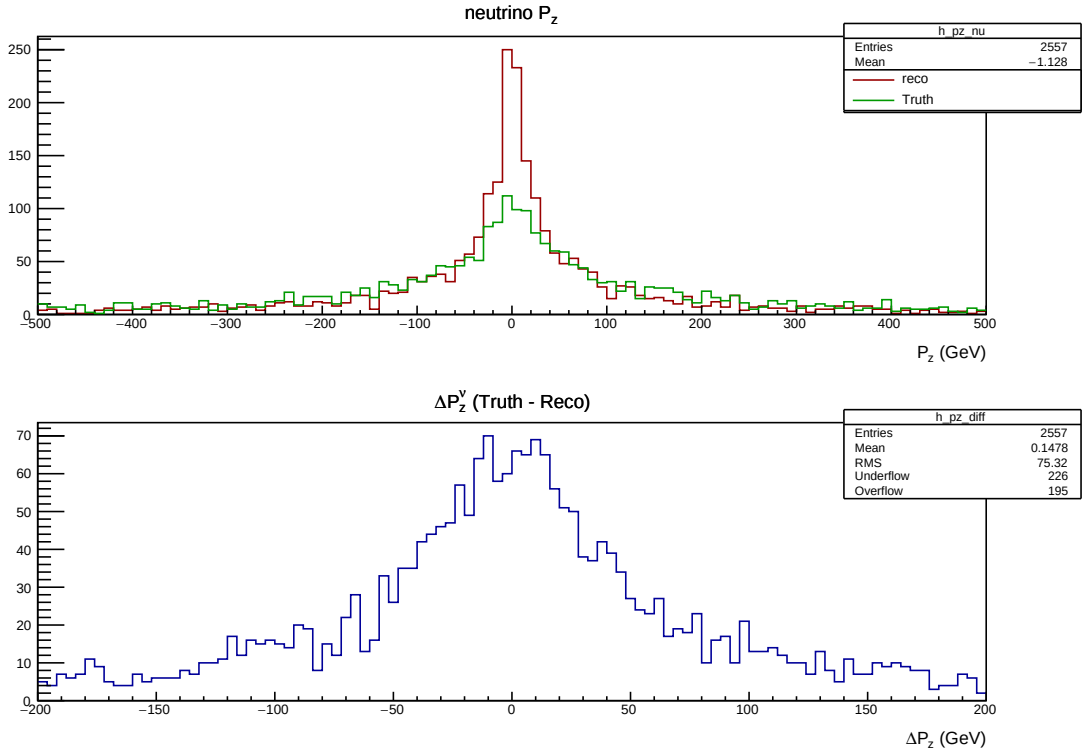

Figure 4.4: Comparison of the calculated $p_{z,\nu}$ to the "Truth" in the case where $\Delta < 0$ and E_T^{miss} has been modified, m(W')=5 TeV, $\sqrt{s} = 13$ TeV.

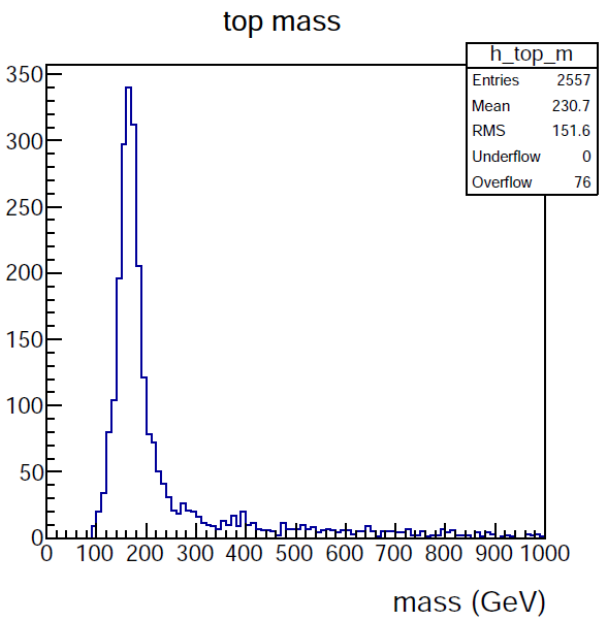

Figure 4.5: Reconstructed top quark mass at $\sqrt{s} = 13$ TeV, m(W')=5 TeV.

4.1.3 Reconstructing the W'

Once the top-quark 4-vector has been built, we need to find the jet corresponding to the b-quark coming from the W' boson decay: $b_{W'}$. In events with more than two jets passing our selection (detailed in section 4.5), this jet is chosen between the remaining as the one with the highest transverse momentum, since the corresponding b-quark comes from the decay of a massive W', and is thus highly energetic. We can finally build our W' boson 4-vector: $P_{W'} = P_{top} + P_{b_{W'}}$.

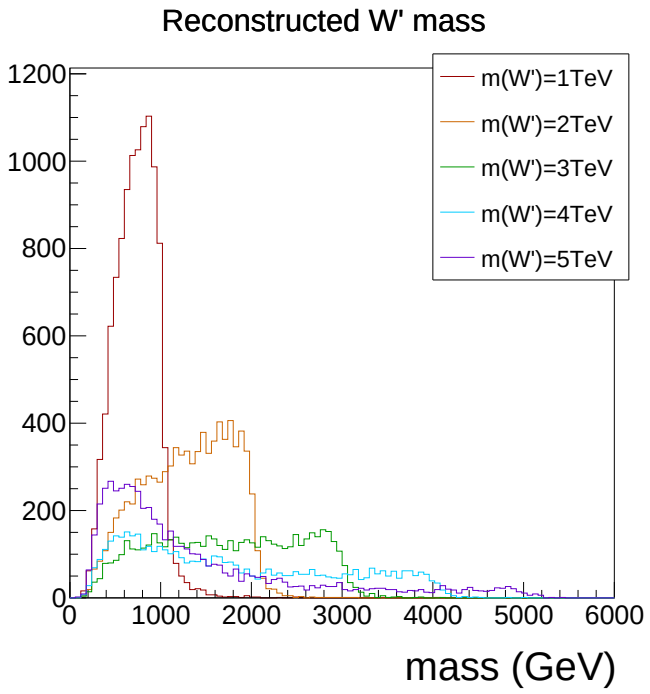

Figure 4.6: Reconstructed W' boson masses at $\sqrt{s} = 13$ TeV, m(W')=1→5 TeV.

Figure 4.6 gives the reconstructed W' boson masses for input masses ranging from 1 to 5 TeV, at $\sqrt{s} = 13$ TeV. As we can see it will be difficult to find the W' boson by reconstructing it this way, if its' mass is greater than 3 TeV. This reconstruction will need many improvements if we want to discover the W' boson this way. This figure looks very much like the distribution of m_{tb}^{Truth} after gluon emissions. It seems that most of the quarks' energy loss due to the emissions has not been recovered in the jets after all. Maybe the first improvement we should bring to this study is to consider larger cones in the reconstruction of jets. The size parameter for this study is R=0.4, an interesting study would be to try larger parameters and see if we obtain a nicer shape of these mass distributions.

Another thing we should improve is the way to find the b_{top} and $b_{W'}$ jets, as detailed in section 4.2, and our reconstruction of the neutrino's longitudinal momentum, we should probably keep the 2 solutions when $\Delta > 0$ and choose the one which gives the best top quark mass as well.

4.2 Matching the b-jets

Another use of the "Truth" is to check if we have found the right b-jet, and thus if our method is accurate. We have done this by drawing histograms of the distance in $\eta - \phi$ space ΔR between the chosen jet and the "Truth" corresponding b-quark. As a reminder, ΔR is defined as $\sqrt{\Delta\eta^2 + \Delta\phi^2}$.

Jets are reconstructed using the anti-k_t algorithm with a radius parameter R=0.4 [48], we have thus considered a jet to be correctly matched if the distance ΔR is smaller than 0.4. Figure 4.7 shows the distributions of this distance between the chosen jets and the "Truth" b-quarks, at $\sqrt{s} = 8$ TeV with a W' boson mass of 3 TeV.

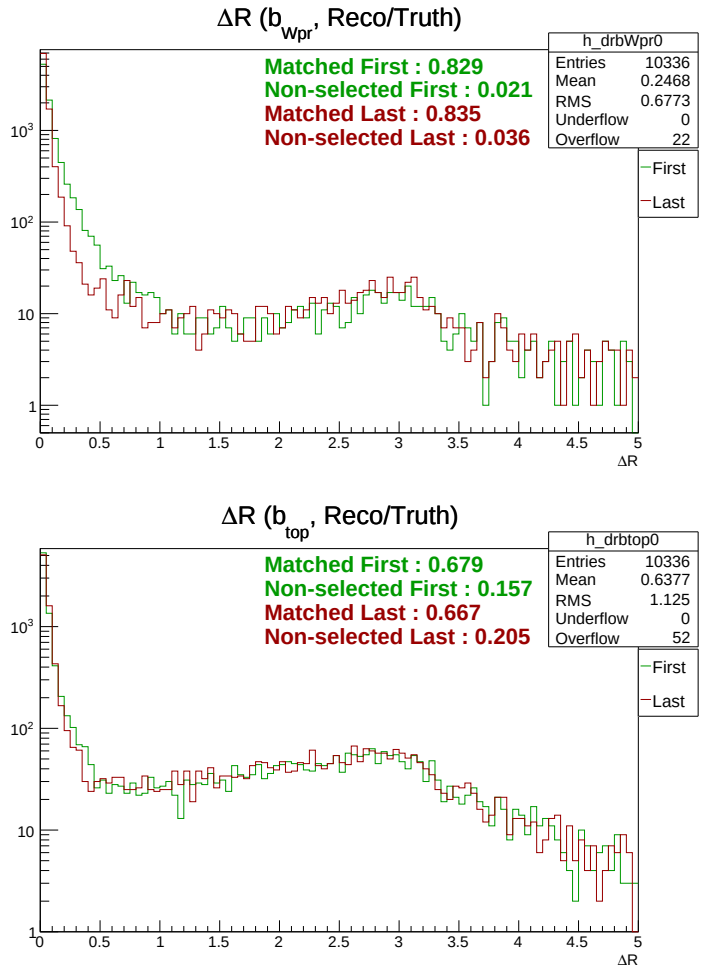

Figure 4.7: ΔR between the chosen jet and corresponding "Truth" quark: $b_{W'}$ and b_{top} at $\sqrt{s} = 8$ TeV, m(W')=3 TeV, "First" concerns the "Truth" quark before gluon emissions, and "Last" after them.

As we can see in this figure, $b_{W'}$ is better matched than b_{top}. This shows us that the method to get b_{top} is not accurate enough, we will need improvements concerning this issue. In this figure, "First" concerns the quark before gluon emission, and "Last" after them. "Non-selected First/Last" concern "Truth" quarks that have not passed our selection criteria, which can for example be the minimum transverse momentum of this quark, and are listed in section 4.4.

For example, if we take the 20.5 % of "Non-selected Last" b_{top} in this figure, this means that 20.5 % of the events have passed our selection without the b-jet coming from the top-quark decay. In this example b_{top} might have emitted many gluons and not be energetic enough to pass our selection. This is a concern for our study, many reconstructed W' bosons may not be reconstructed with the right jets. At $\sqrt{s} = 13$ TeV, jets tend to be highly energetic but there are no less of these cases, and the matching of b_{top} and $b_{W'}$ remains an issue, as shown in Table 4.1.

In this table, only the "Last" quarks have been put since these are the ones we would reconstruct in the detector. We must keep in mind that the reconstructed jet in the detector does not only have the energy of the b-quark, and thus some of the non-selected quarks in the table above will be selected if the transverse momentum is the criterion that failed the selection.

W' boson mass (TeV)	**matched** $b_{W'}$ (%)	**non-selected** $b_{W'}^{Truth}$ (%)	**matched** b_{top} (%)	**non-selected** b_{top}^{Truth} (%)
1	90.5	6.5	69.4	17.9
2	88.6	8.4	53.3	15.9
3	80.3	16.6	48.2	15.7
4	56.3	41.4	53.4	16.1
5	35.8	59.9	60.7	15.7

Table 4.1: Matching and selection percentages for $b_{W'}$ and b_{top} for m(W')=1→5 TeV, at $\sqrt{s} = 13$ TeV.

4.3 Backgrounds

Backgrounds have a similar final state to our signal, and can thus be reconstructed and compromise the study. In this section we will briefly go through the major backgrounds to our signal. They have not all been thoroughly considered in our studies, we have concentrated on the most abundant ones.

4.3.1 $t\bar{t}$ production

This background is the most abundant one to our signal. Studies shown in this report will only concern this process, because of its' abundance.

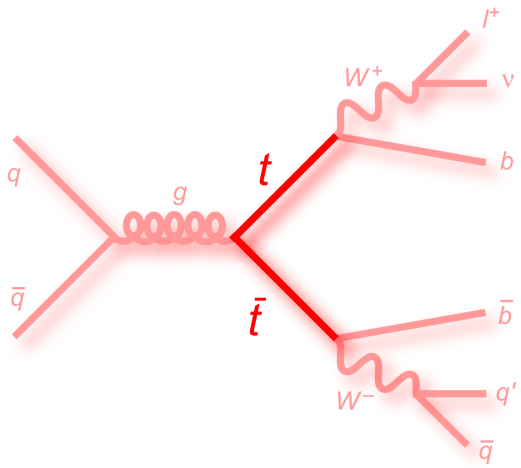

Figure 4.8: Feynman diagram of a $t\bar{t}$ pair production in the semi-leptonic final state.

Figure 4.8 shows the Feynman diagram of a $t\bar{t}$ pair production in the semi-leptonic final state. As we have seen in chapter 1, almost 90 % of its' production corresponds to gluon fusion and thus not to this Feynman diagram, but the final state is the same. As we can see this process almost has the same final state than the researched signal, and will pass our selection if one or two of its' jets do not pass it. Furthermore at run II $t\bar{t}$ pairs can be *boosted* and thus have an important invariant mass, which makes it likely to have highly energetic objects in its' final state.

4.3.2 Other backgrounds

Another background which has been seen in chapter 1 is the single-top production, and is the second most abundant background, due to its' three production channels: s, t and tW. The s-channel has exactly the same final state as the researched signal, but has a low cross-section of production. These processes have final states which could pass our selection, but the objects are not as energetic as for our signal, they can be easily discriminated.

Multijets processes are also a very abundant background, which consist in quark annihilation into a gluon or in gluon fusion, that give processes with only quarks, thus jets. These processes don't include a neutrino, criteria concerning the missing transverse energy can reject them efficiently.

Other backgrounds are W+jets, Z+jets and Diboson events which are maybe not as numerous as the $t\bar{t}$ production, but still need to be taken into account and controlled, for we will want to have the best signal over background ratio possible, which is only possible if we perfectly know our backgrounds.

4.4 A new opportunity?

In this study, we have illustrated the increased probability of producing a W' boson at run II in our simulation of the reconstruction of events in the detector by drawing histograms of differential cross sections, function of m_{tb}^{Reco}, the reconstructed invariant mass of the $\{\text{top}+\bar{b}\}$ system: $\frac{d\sigma}{dm_{tb}^{Reco}}$.

These histograms correspond to reconstructed mass spectra normalised to the corresponding theoretical cross-sections.

Figure 4.9 shows the cross-section for the $pp \to W' \to tb$ process in each bin of the reconstructed $\{\text{top}+\bar{b}\}$ invariant mass. Histograms have been made at both centre of mass energies and divided, in order to confirm the increased cross-section between 8 and 13 TeV collisions. This figure shows the ratio for a W' mass of 3 TeV.

As we can see, for m_{tb}^{Reco} between 2 and 3 TeV, the production rate will be multiplied by a factor around 15, thus the great opportunity brought by the run II. The effect is even larger for higher masses, since the production of a W' boson with a mass higher than 3 TeV at $\sqrt{s} = 8$ TeV becomes negligible.

This increased potential is not the only aspect we must consider, there are also the backgrounds corresponding to the searched final state. In this particular study we have considered the $t\bar{t}$ pair production. We have done the same study for this dominant background as we have for the signal, reconstructed it as if it were the researched signal and drawn differential cross-sections at both centre of mass energies to obtain the ratio. This gives the increased potential for producing $t\bar{t}$ pairs which can be mistaken for the W' signal we are searching for during run II. This is illustrated in Figure 4.10.

This reconstruction is exactly the same as the one we have done with the signal to obtain the W' boson, except that the input data samples are $t\bar{t}$ production samples. This figure shows that the $t\bar{t}$ cross-section is also greatly increased for high masses of the $\{\text{top}+\bar{b}\}$ system. The production rate will be multiplied by a factor roughly the same as that of the signal, which is a concern. This aspect will need to be controlled, and the selection criteria which discriminate the researched signal from backgrounds need to be optimised to this energy range.

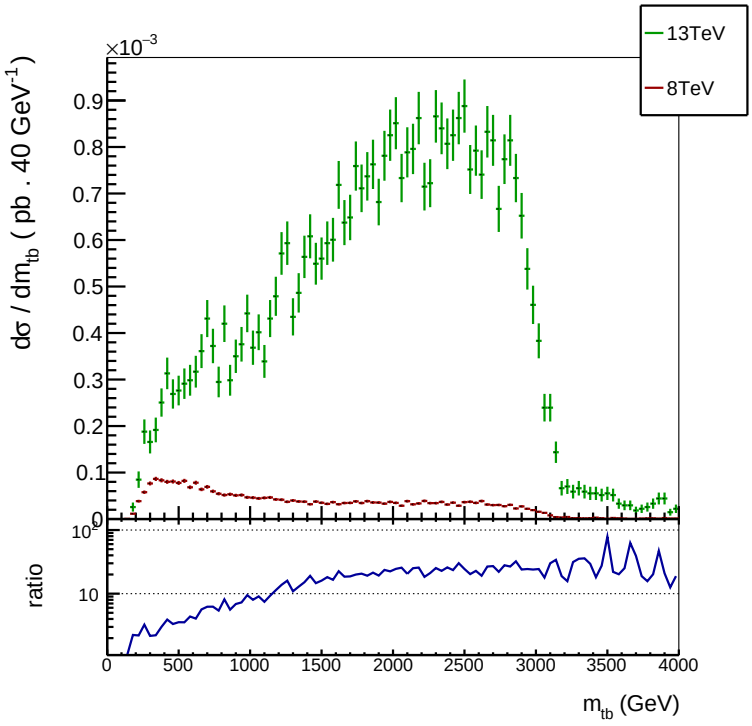

Figure 4.9: Differential cross-sections at $\sqrt{s} = 8/13$ TeV and their ratio, m(W')=3 TeV.

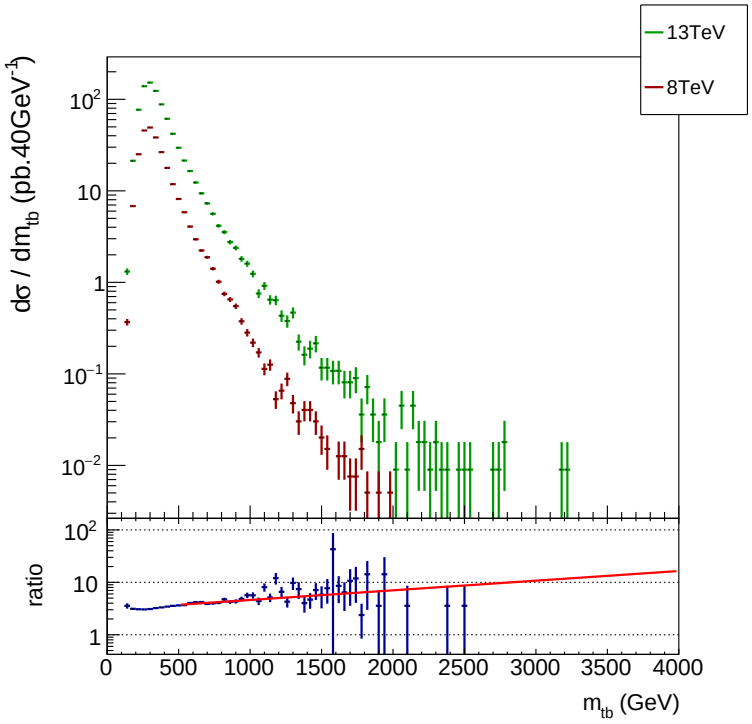

Figure 4.10: Differential cross-sections of the $t\bar{t}$ production at $\sqrt{s} = 8/13$ TeV and their ratio.

4.5 Selection criteria

In our reconstruction, we must establish selection criteria to discriminate our signal from the backgrounds. In these studies, we have used the same selection criteria than those that were used for the research with data from run I [49]. These consist in selecting object and event characteristics which should be representative of the researched signal, as highly energetic objects since we are looking for a massive W' boson, and angular distributions which can be measured in the ATLAS detector. There are criteria on objects as well as on events.

For electrons: $p_T > 30$ GeV; $|\eta| < 2.5$, with a veto corresponding to a non-instrumented part of the detector, where the cables are: $1.37 < |\eta| < 1.52$. For muons: $p_T > 30$ GeV; $|\eta| < 2.5$; and for jets: $p_T > 25$ GeV; $|\eta| < 2.5$.

The criteria on events are the following, there must be 2 or 3 jets that pass the criterion in the event, with at least one of them identified as coming from a b-quark (b-tagged). The missing transverse momentum must be over: $E_T^{miss} > 35$ GeV, and there is another criterion concerning the missing energy: W-boson transverse mass : $m_T(W) + E_T^{miss} > 60$ GeV:

$$m_T(W) = \sqrt{(P_{T,l} + P_{T,\nu})^2 - (P_{x,l} + P_{x,\nu})^2 - (P_{y,l} + P_{y,\nu})^2}.$$

4.6 Improvements for $\sqrt{s} = 13$ TeV

In this study we have looked to optimise these criteria for run II, as well as find some new ones which could also be efficient against the backgrounds, especially the $t\bar{t}$ production.

4.6.1 Selection criteria optimisation

To optimise the criteria we have from the previous research, we have taken them from the list above, and simply made them vary step by step and looked at the number of events that had passed them for the signal and background. We have done this by looking at a particular value, which we have called s for the signal and B for the $t\bar{t}$ background:

$$s = \sigma \epsilon L$$

where σ is the process cross-section, $\epsilon = \frac{N_{pass}}{N_{total}}$ is the efficiency and L is the integrated luminosity.

We have drawn distributions of s and B to have the impact of a given criterion on the signal and background, but also $\frac{s}{B}$, $\frac{s}{\sqrt{B}}$, $\frac{s}{\sqrt{B \oplus 10\% B}}$ and $\frac{s}{\sqrt{B \oplus 20\% B}}$.

We have done this in order to obtain the best region for a given criterion, and have also done this with two criteria at a time to take into account the correlations. An example of this study is given in Figure 4.11 where $\frac{s}{\sqrt{B \oplus 10\% B}}$ and $\frac{s}{\sqrt{B \oplus 20\% B}}$ are plotted for the two following criteria: the leading jet minimum tansverse momentum versus the minimum missing transverse energy, at $\sqrt{s} = 13$ TeV and m(W')=3 TeV.

This study has shown that we must increase the selection criteria that has been used for the research at $\sqrt{s} = 8$ TeV in order to have an acceptable signal over background ratio, many more studies like this one will need to have some thought put into for us to be ready for the run II data.

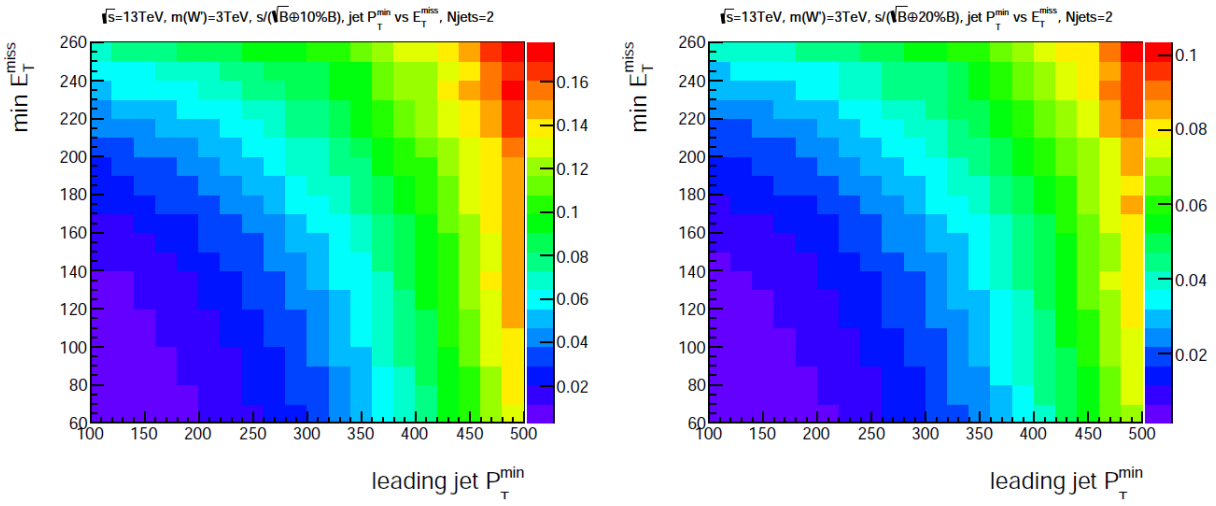

Figure 4.11: Optimisation of the two criteria: leading jet minimum tansverse momentum versus minimum missing transverse energy, at $\sqrt{s} = 13$ TeV and m(W')=3 TeV.

4.6.2 New criteria

Many new criteria could help improve our selection for run II. One has been found by trying new kinematical distributions, which could prove to be useful. To tell if a criterion is efficient, we do the following: make it increase step-by-step and calculate the efficiency:

$$\epsilon = \frac{N_{pass}}{N_{total}}$$

for the signal and background, and draw signal versus background efficiency, as shown in Figure 4.12 for the new criterion we have tested.

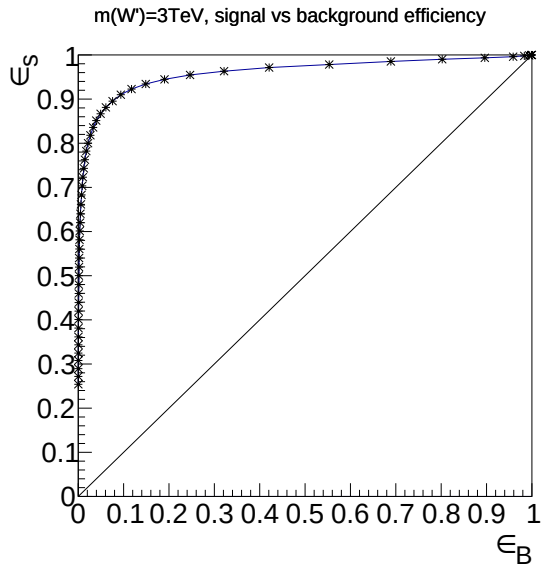

Figure 4.12: Efficiency test of a new criterion: $P_T^{jet_1,jet_2}$, for m(W')=3 TeV vs $t\bar{t}$ at $\sqrt{s} = 13$ TeV.

To each point on the curve corresponds an increase of this criterion, which is the minimum transverse momentum of the vector sum of the two leading jets:

$$min(P_T^{\overrightarrow{jet_1}+\overrightarrow{jet_2}})$$

(which should correspond to b_{top} and $b_{W'}$). It is shown here with the signal at $\sqrt{s} = 13$ TeV and W' boson mass of 3 TeV against the $t\bar{t}$ background. We have also tested this new criterion against the single-top background and it has proven to be very efficient.

For a criterion to be considered efficient, we look at the area between the curve and diagonal, which must be the largest possible. As seen in this figure, this criterion could reject up to 90 % of the $t\bar{t}$ background while only rejecting less than 10 % of the signal, it could prove to be very useful for run II. A set of selection criteria will be tested in the future studies to come, and their ranking will be directly linked to the area between their efficiency curve and the diagonal.

Conclusion & future prospects

We have studied simulated data of $W' \to t\bar{b}$ decays as would happen during run II at LHC. We first briefly went through the theoretical and experimental contexts, explaining what leads to this research and what are its' goals, and then we went through the studies that have been made during this internship. These studies have been split into two main parts.

The first part deals with studies at the parton level, where we have introduced the Monte Carlo generators used to create the data samples on which our studies were made. We then explained the impact of parton distribution functions and of gluon emissions by the top and b-quarks on the invariant mass of the top plus b-quark system, and thus on the reconstructed mass of the W' boson. We have shown that these physics aspects would complicate the search for this new particle. Finally, we described the increased potential for discovery of the W' boson with two aspects, such a heavy particle could not be produced at a centre of mass energy $\sqrt{s}$ of 8 TeV, in some part due to parton distribution functions, but an increase in the collision energy can make its' production possible and will increase the cross-section of the $pp \to W' \to t\bar{b}$ process.

In the second part, we detailed the steps to the reconstruction of the W' boson 4-vector in a detector simulation. We pointed out the difficulties we encountered, and some possible areas in which we can improve the reconstruction. We have indeed seen the method for building the neutrino 4-vector and the way to identify each b-jet to the corresponding decay, the top quark or the W' boson. This matching needs to be improved, especially for high masses of the W' boson. We have also brought up an improvement for studies at partonic and detector levels, which would be to use a larger radius parameter for the reconstruction of jets, since at higher energies the quarks will radiate more gluons. A larger radius could enable us to limit the energy loss due to these emissions. It would as well enable a better selection of jets in our selection criteria, which we have also looked to improve. These discriminations of signal from backgrounds need to be optimised for the 13 TeV centre of mass energy, and we have shown how some criteria will be improved and how some new criteria have been tested.

Searches at $\sqrt{s} = 8$ TeV have not observed significant deviations from the Standard Model expectations and have set a lower limit to the W' boson mass to 2.05 TeV at 95% confidence level. We can only hope to observe significant deviations from the Standard Model at $\sqrt{s} = 13$ TeV, but we shall expect to improve the exclusions made on this particle's mass and other characteristics. These studies have shown that there is much left to do before a W' boson can be found in this decay channel, but that there is a great potential with the upcoming run II for the discovery of this new particle. Its' discovery could prove that the Standard Model is correct at the energy scales at which it has been probed until now, but is part of a bigger model which could help answer to many questions left open in particle physics today.

Bibliography

[1] K.A. Olive et al. Review of Particle Physics. *Chin.Phys.*, C38:090001, 2014.

[2] First combination of Tevatron and LHC measurements of the top-quark mass, 2014.

[3] A. Pich. Quantum chromodynamics, 1995.

[4] S.L. Glashow. Partial Symmetries of Weak Interactions. *Nucl.Phys.*, 22:579–588, 1961.

[5] Steven Weinberg. A Model of Leptons. *Phys.Rev.Lett.*, 19:1264–1266, 1967.

[6] F. Englert and R. Brout. Broken symmetry and the mass of gauge vector mesons. *Phys. Rev. Lett.*, 13:321–323, Aug 1964.

[7] Peter W. Higgs. Broken symmetries, massless particles and gauge fields. *Phys.Lett.*, 12:132–133, 1964.

[8] Peter W. Higgs. Broken Symmetries and the Masses of Gauge Bosons. *Phys.Rev.Lett.*, 13:508–509, 1964.

[9] Georges Aad et al. Observation of a new particle in the search for the Standard Model Higgs boson with the ATLAS detector at the LHC. *Phys.Lett.*, B716:1–29, 2012.

[10] Serguei Chatrchyan et al. Observation of a new boson at a mass of 125 GeV with the CMS experiment at the LHC. *Phys.Lett.*, B716:30–61, 2012.

[11] Georges Aad et al. Evidence for the spin-0 nature of the Higgs boson using ATLAS data. *Phys.Lett.*, B726:120–144, 2013.

[12] Serguei Chatrchyan et al. Study of the Mass and Spin-Parity of the Higgs Boson Candidate Via Its Decays to Z Boson Pairs. *Phys.Rev.Lett.*, 110(8):081803, 2013.

[13] Updated coupling measurements of the Higgs boson with the ATLAS detector using up to 25 fb^{-1} of proton-proton collision data. Technical Report ATLAS-CONF-2014-009, CERN, Geneva, Mar 2014.

[14] Combined measurements of the mass and signal strength of the Higgs-like boson with the ATLAS detector using up to 25 fb^{-1} of proton-proton collision data, 2013.

[15] Frank-Peter Schilling. Top Quark Physics at the LHC: A Review of the First Two Years. *Int.J.Mod.Phys.*, A27:1230016, 2012.

[16] Commissioning of the ATLAS high-performance b-tagging algorithms in the 7 TeV collision data. 2011.

[17] Ehab Malkawi, Timothy M.P. Tait, and C.P. Yuan. A Model of strong flavor dynamics for the top quark. *Phys.Lett.*, B385:304–310, 1996.

[18] David J. Muller and Satyanarayan Nandi. Top flavor: A Separate SU(2) for the third family. *Phys.Lett.*, B383:345–350, 1996.

[19] Xu-Feng Wang, Chun Du, and Hong-Jian He. LHC Higgs Signatures from Topflavor Seesaw Mechanism. *Phys.Lett.*, B723:314–323, 2013.

[20] Stephen P. Martin. A Supersymmetry primer. *Adv.Ser.Direct.High Energy Phys.*, 21:1–153, 2010.

[21] M. Roos. Dark Matter: The evidence from astronomy, astrophysics and cosmology. *ArXiv e-prints*, January 2010.

[22] T. Abbott et al. The dark energy survey. 2005.

[23] Search for direct top squark pair production in final states with one isolated lepton, jets, and missing transverse momentum in $sqrts = 8$,TeV pp collisions using 21 fb^{-1} of ATLAS data. 2013.

[24] Theodor Kaluza. On the Problem of Unity in Physics. *Sitzungsber.Preuss.Akad.Wiss.Berlin (Math.Phys.)*, 1921:966–972, 1921.

[25] Oskar Klein. Quantum Theory and Five-Dimensional Theory of Relativity. (In German and English). *Z.Phys.*, 37:895–906, 1926.

[26] Nima Arkani-Hamed, Savas Dimopoulos, and G.R. Dvali. The Hierarchy problem and new dimensions at a millimeter. *Phys.Lett.*, B429:263–272, 1998.

[27] Kaustubh Agashe, Alexander Belyaev, Tadas Krupovnickas, Gilad Perez, and Joseph Virzi. LHC Signals from Warped Extra Dimensions. *Phys.Rev.*, D77:015003, 2008.

[28] Howard Georgi and S. L. Glashow. Unity of all elementary-particle forces. *Phys. Rev. Lett.*, 32:438–441, Feb 1974.

[29] A. Pomarol. Beyond the Standard Model. 2012.

[30] Gustavo Burdman, Bogdan A. Dobrescu, and Eduardo Ponton. Resonances from two universal extra dimensions. *Phys.Rev.*, D74:075008, 2006.

[31] Hsin-Chia Cheng, Christopher T. Hill, Stefan Pokorski, and Jing Wang. The Standard model in the latticized bulk. *Phys.Rev.*, D64:065007, 2001.

[32] Thomas Appelquist, Hsin-Chia Cheng, and Bogdan A. Dobrescu. Bounds on universal extra dimensions. *Phys.Rev.*, D64:035002, 2001.

[33] Jogesh C. Pati and Abdus Salam. Lepton Number as the Fourth Color. *Phys.Rev.*, D10:275–289, 1974.

[34] Rabindra N. Mohapatra and Jogesh C. Pati. Left-Right Gauge Symmetry and an Isoconjugate Model of CP Violation. *Phys.Rev.*, D11:566–571, 1975.

[35] Maxim Perelstein. Little Higgs models and their phenomenology. *Prog.Part.Nucl.Phys.*, 58:247–291, 2007.

[36] V.M. Abazov et al. Search for W' bosons decaying to an electron and a neutrino with the D0 detector. *Phys.Rev.Lett.*, 100:031804, 2008.

[37] T. Aaltonen et al. Search for a New Heavy Gauge Boson W' with Electron + missing ET Event Signature in $p\bar{p}$ collisions at $\sqrt{s} = 1.96$ TeV. *Phys.Rev.*, D83:031102, 2011.

[38] Georges Aad et al. Search for new particles in events with one lepton and missing transverse momentum in pp collisions at $\sqrt{s} = 8$ TeV with the ATLAS detector. *JHEP*, 1409:037, 2014.

[39] Victor Mukhamedovich Abazov et al. Search for $W' \to tb$ resonances with left- and right-handed couplings to fermions. *Phys.Lett.*, B699:145–150, 2011.

[40] T. Aaltonen et al. Search for the Production of Narrow t anti-b Resonances in 1.9 fb-1 of p anti-p Collisions at s**(1/2) = 1.96-TeV. *Phys.Rev.Lett.*, 103:041801, 2009.

[41] Georges Aad et al. Search for tb resonances in proton-proton collisions at $\sqrt{s} = 7$ TeV with the ATLAS detector. *Phys.Rev.Lett.*, 109:081801, 2012.

[42] Serguei Chatrchyan et al. Search for W' → tb decays in the lepton + jets final state in pp collisions at $\sqrt{s} = 8$ TeV. *JHEP*, 1405:108, 2014.

[43] Georges Aad et al. Search for $W' \to tb \to qqbb$ decays in pp collisions at $\sqrt{s} = 8$ TeV with the ATLAS detector. *Eur.Phys.J.*, C75(4):165, 2015.

[44] Johan Alwall, Michel Herquet, Fabio Maltoni, Olivier Mattelaer, and Tim Stelzer. MadGraph 5 : Going Beyond. *JHEP*, 1106:128, 2011.

[45] Torbjorn Sjostrand, Stephen Mrenna, and Peter Z. Skands. A Brief Introduction to PYTHIA 8.1. *Comput.Phys.Commun.*, 178:852–867, 2008.

[46] J. de Favereau et al. DELPHES 3, A modular framework for fast simulation of a generic collider experiment. *JHEP*, 1402:057, 2014.

[47] A.D. Martin, W.J. Stirling, R.S. Thorne, and G. Watt. Parton distributions for the lhc. *The European Physical Journal C*, 63(2):189–285, 2009.

[48] Matteo Cacciari, Gavin P. Salam, and Gregory Soyez. The Anti-k(t) jet clustering algorithm. *JHEP*, 0804:063, 2008.

[49] Search for $W' \to t\bar{b}$ in the lepton plus jets final state in proton–proton collisions at a centre-of-mass energy of $\sqrt{s} = 8$ TeV with the ATLAS detector. *Physics Letters B*, 743(0):235 – 255, 2015.

Abstract

Despite its' 40 years of experimental success, the Standard Model, a theory which describes fundamental particles as well as three fundamental interactions, has theoretical and experimental limitations. These lead to the existence of theories beyond the Standard Model, called New Physics. This report presents the search for a new particle present in many theories beyond the Standard Model: the W' boson.

This year, the Large Hadron Collider is entering run II, which will see proton-proton collisions take place at an unprecedented centre of mass energy of 13 TeV. This high energy will provide the mouth watering prospect of finding New Physics.

Studies that have been made during this internship have used Monte Carlo simulations of events that we should see in the ATLAS detector at LHC during run II. These studies are grouped into two main parts.

The first part consists in studies at the parton level, where we see the impact of physics aspects as parton distribution functions and gluon radiations by quarks on the reconstructed mass of the W' boson. We also see the increased potential for discovery of this new particle by comparing invariant mass distributions and cross-sections at centre of mass energies of 8 TeV and 13 TeV.

The second part describes the step-by-step reconstruction of the W' boson in a detector simulation. The main difficulties in these steps are pointed out, as well as several ideas for improvements for run II. Background processes and the selection criteria that have been used to discriminate them from the signal are introduced, and optimisations of these criteria as well as efficiency tests for new ones are presented.

This search is the sequel to a large number of studies made during run I, and will look to continue to improve the seek for beyond the Standard Model particles.

Résumé

Malgré ses 40 ans de succès expérimentaux, le Modèle Standard, théorie décrivant les particules élémentaires et trois des interactions fondamentales, souffre de difficultés théoriques et expérimentales. Ces dernières mènent à l'existence de théories au-delà du Modèle Standard, dites de Nouvelle Physique. Ce rapport présente la recherche d'une nouvelle particule présente dans un grand nombre de théories au-del'a du Modèle Standard : le boson W'.

Cette année, le Grand Collisionneur de Hadrons (LHC) entame son run II, où l'on verra des collisions proton-proton à une énergie dans le centre de masse inédite de 13 TeV. Cette grande énergie nous apportera la perspective excitante de voir de la Nouvelle Physique.

Les études menées durant ce stage ont été faites sur des simulations Monte Carlo d'évènements que l'on devrait voir au sein du détecteur ATLAS au run II du LHC. Ces études sont groupées en deux grandes parties.

La première partie consiste en des études au niveau partonique, où l'on voit l'impact d'aspects physiques tels que les fonctions de densité partonique et les émissions de gluons par les quarks sur la masse reconstruite du boson W'. On y voit aussi le potentiel accru de découverte de cette nouvelle particule en comparant des spectres de masse invariante ainsi que des sections efficaces aux énergies dans le centre de masse de 8 TeV et 13 TeV.

La seconde partie décrit les étapes de la reconstruction du boson W' dans une simulation de détecteur. Les étapes présentant les plus grandes difficultés sont mises en valeur, ainsi que quelques idées d'améliorations pour le run II. Les processus de bruit de fond et les critères de sélection utilisés pour les discriminer par rapport au signal sont introduits, et les optimisations de ces critères ainsi que les tests d'efficacité pour en trouver de nouveaux sont présentés.

Cette recherche est la suite d'un grand nombre d'études faites durant le run I, elle cherchera à continuer d'améliorer la recherche de particules au-delà du Modèle Standard.